Article no. 22

THE CIVIL ENGINEERING JOURNAL 2-2019

DESIGNS FOR T SHAPE FISHWAYS

Xi Mao[1,2,] , Jiehao Zhang[1], Kai Tang[1], Weiyang Zhao[2]*

1. *Sichuan Agricultural University, College of Water Conservancy and Hydropower Engineering, Yaan, Road Xinkang 46, China; maowhiteknight@163.com*
2. *Water Research Laboratory, School of Civil and Environmental Engineering, The University of New South Wales, Sydney, King Street 110, Australia*

ABSTRACT

This paper presented results of a numerical study on seven designs of T shape fishways. The trajectory equation of the maximum velocity line and the V/V_a equation of the T shape fishways were obtained from the results. It was found that a width of $1.5b_s$ for the T lateral baffle, a width of $5b_s$ and a length of $6.25b_s$ for the pools were very satisfactory for the dimensional design of T shape fishways, where b_s was the slot width. From the seven designs studied, design 3 (D3, D denotes "design") was recommended for practical use.

KEYWORDS

Fishway, Civil engineering measures, Hydrodynamics, Hydraulics, Numerical simulation

INTRODUCTION

Fishways (or fish passes, fish passages) are structures that facilitate the upstream or downstream migration of aquatic organisms over obstructions to migration such as dams and weirs. Although constructing fishways does not eliminate the basic ecological damage caused by dams, such as loss of river habitat or loss of longitudinal connectivity, this measure attenuates the negative ecological impact of these obstructions to a certain extent, and thereby increases their ecological compatibility [1], [2].

Three types of technical fishways are commonly used in engineering:

(1) Denil fishways [3], [4], [5]
(2) pool and weir fishways [6], [7], [8]
(3) vertical slot fishways [9], [10], [11]

The Denil fishway is impressionable to fluctuating water levels and is prone to clogging up with silt and debris, so it needs to operate at higher water levels than other types of fishways. The pool and weir fishway is inadaptable to large water level fluctuations, and does not allow fish passing across the entire cross section. The vertical slot fishway is adaptable to frequent water level fluctuations, and allows fish to pass across the entire cross section and is not prone to be blockage. Another problem arises, however, which is that the velocity is extremely high in some areas, such as vertical slot zone.

Mao et al [12] first put forward a new kind of fishway called a T shape fishway by means of numerical simulation and physical experimentation. The T shape fishway consists of consecutive and identical pools, and includes a series of inlet lateral baffles and T shape baffles. The T shape baffle is named for its shape, which is composed of the T lateral baffle and the T central baffle.

Compared to these three traditional technical fishway types, the T shape fishway has plane symmetry, and the following obvious features:

(1) it can meet the migratory requirements of these fish with poor swimming and jumping capability, in terms of velocity and flow pattern

(2) the main flow travels from one slot to the next through the pool as a two-dimensional curved flow with gentle slope (S≤10%), where S is the slope of the fishway [9], [12].

This paper aims to understand the hydraulics of the T shape fishway, to develop simpler pool designs by means of numerical simulation.

METHODS

A commercial CFD solver (Fluent) was used to create a numerical model to solve the optimal control problem related to the optimal management of T shape fishways. The mathematical model uses the finite-volume method to solve the three-dimensional Navier-Stokes equation using the standard k-ε turbulence model. Complete details of the mathematical model, including the solution method, boundary conditions, and mesh conditions, is provided in works by Mao *et al*. By using the experimental method, the mathematical model was validated by Mao *et al*, and it was found that the rationality of the numerical simulation and experiments validate the overall controlling error within 8% [12].

Numerical simulation

Seven designs of T shape fishways were studied by using numerical simulation. These seven T shape fishway models were all set in the same water channel, with 24.5 m long, 2.0 m wide, and 1.2 m high. Baffles were set vertically within the water channel for each design with the slope of the flume set as S=2.6%. In each design, there were six regular pools in the flume, with two transition pools, one at the beginning of the water channel and the other at the end. The flow discharge in each design was Q=400 L/s. Figures 1 (a) and (b) show the details of the seven designs.

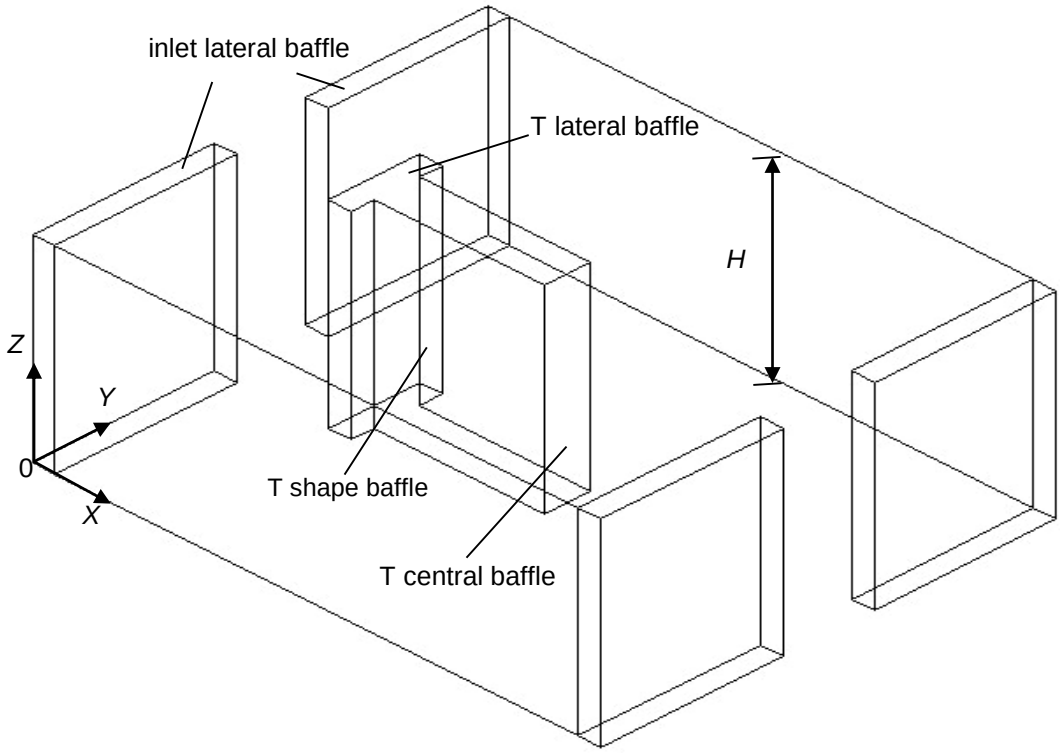

Fig. 1 (a) – Three-dimensional stereogram of fishway designs considered in this study

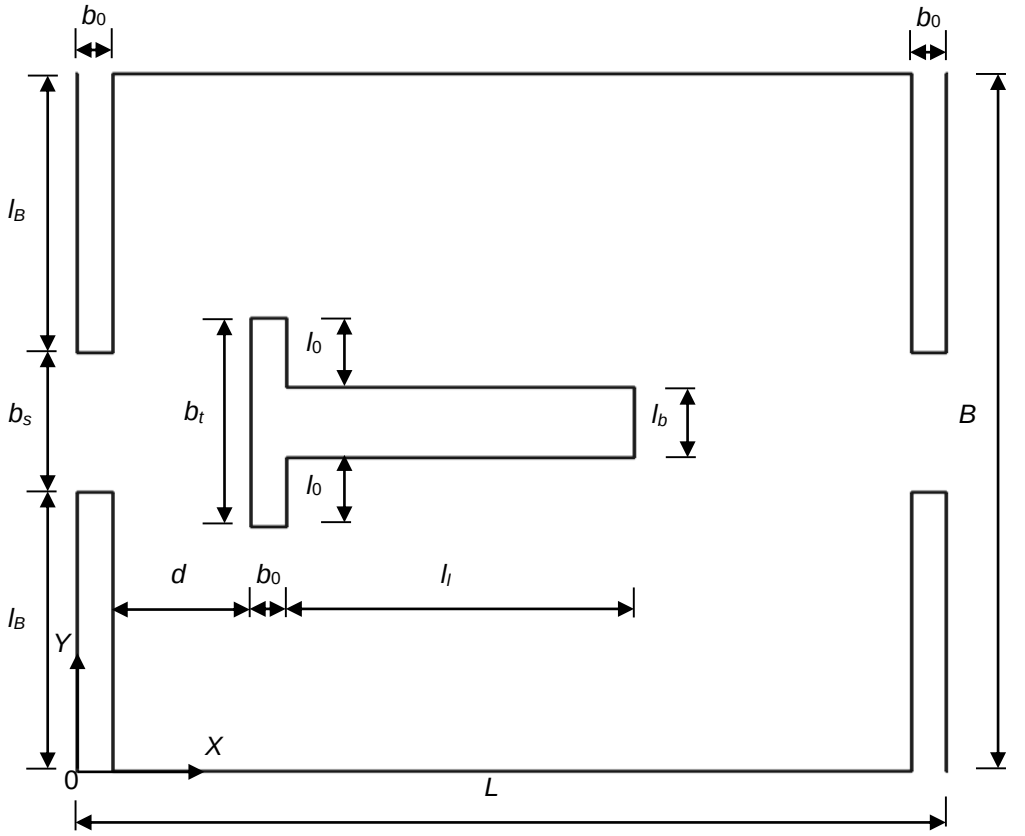

Fig 1 (b) – Planar graph of fishway designs considered in this study

The sizes of all of the seven designs in this study are shown in Table 1, where *L*, *B*, and *H* represent the length, width, and height of the single regular pool, respectively. b_s is the width of the slot, l_B is the length of the lateral baffle, and b_0 is the width of the inlet lateral baffle and the T lateral baffle. l_l and l_b represent the length and the width of the T central baffle, respectively. b_t is the length of the T lateral baffle, and *d* is the distance between the slot and the T lateral baffle.

Tab. 1- Sizes of the seven fishway designs under study (D denotes "design")

D	l_l (m)	l_b (m)	l_B (m)	b_0 (m)	b_s (m)	*B* (m)	*H* (m)	b_t (m)	l_0 (m)	*d* (m)	*L* (m)	*B*/*L*
1	1.0	0.2	0.8	0.1	0.4	2.0	1.2	0.6	0.2	0.4	3.0	2/3
2								0.6	0.2	0.4	2.0	1/1
3								0.6	0.2	0.4	2.5	4/5
4								0.4	0.1	0.4	2.5	4/5
5								0.8	0.3	0.4	2.5	4/5
6								0.6	0.2	0.2	2.5	4/5
7								0.6	0.2	0.6	2.5	4/5

DOI 10.14311/CEJ.2019.02.0022

Numerical models

The governing equations in numerical models include the continuity, momentum, and *k-ε* equations [13], [14]. In this paper, the water density ρ was assumed to be a constant, ρ =10^3 kg/m^3.

The continuity equation is written as:

$$\frac{\partial u}{\partial x}+\frac{\partial v}{\partial y}+\frac{\partial w}{\partial z}=0 \quad (1)$$

The momentum equations as:

$$\frac{\partial u}{\partial t}+u\frac{\partial u}{\partial x}+v\frac{\partial u}{\partial y}+w\frac{\partial u}{\partial z}=-\frac{1}{\rho}\frac{\partial p}{\partial x}+(\mu+\mu_t)(\frac{\partial^2 u}{\partial x^2}+\frac{\partial^2 u}{\partial x\partial y}+\frac{\partial^2 u}{\partial x\partial z}) \quad (2)$$

$$\frac{\partial v}{\partial t}+u\frac{\partial v}{\partial x}+v\frac{\partial v}{\partial y}+w\frac{\partial v}{\partial z}=-\frac{1}{\rho}\frac{\partial p}{\partial y}+(\mu+\mu_t)(\frac{\partial^2 v}{\partial x\partial y}+\frac{\partial^2 v}{\partial y^2}+\frac{\partial^2 v}{\partial y\partial z}) \quad (3)$$

$$\frac{\partial w}{\partial t}+u\frac{\partial w}{\partial x}+v\frac{\partial w}{\partial y}+w\frac{\partial w}{\partial z}=g-\frac{1}{\rho}\frac{\partial p}{\partial z}+(\mu+\mu_t)\left(\frac{\partial^2 w}{\partial x\partial z}+\frac{\partial^2 w}{\partial y\partial z}+\frac{\partial^2 w}{\partial z^2}\right) \quad (4)$$

And the *k-ε* equation as:

$$\frac{\partial k}{\partial t}+u\frac{\partial k}{\partial x}+v\frac{\partial k}{\partial y}+w\frac{\partial k}{\partial z}=\frac{\partial}{\partial x}\left(\frac{\mu_t}{\sigma_k}\frac{\partial k}{\partial x}\right)+\frac{\partial}{\partial y}\left(\frac{\mu_t}{\sigma_k}\frac{\partial k}{\partial y}\right)+\frac{\partial}{\partial z}\left(\frac{\mu_t}{\sigma_k}\frac{\partial k}{\partial z}\right)+\frac{G_k}{\rho}-\varepsilon \quad (5)$$

$$\frac{\partial \varepsilon}{\partial t}+u\frac{\partial \varepsilon}{\partial x}+v\frac{\partial \varepsilon}{\partial y}+w\frac{\partial \varepsilon}{\partial z}=\frac{\varepsilon}{k}C_{1\varepsilon}\frac{G_k}{\rho}-C_{2\varepsilon}\frac{\varepsilon^2}{k}+\frac{\partial}{\partial x}\left[\left(\mu+\frac{\mu_t}{\sigma_\varepsilon}\right)\frac{\partial \varepsilon}{\partial x}\right]+\frac{\partial}{\partial y}\left[\left(\mu+\frac{\mu_t}{\sigma_\varepsilon}\right)\frac{\partial \varepsilon}{\partial y}\right]$$
$$+\frac{\partial}{\partial z}\left[\left(\mu+\frac{\mu_t}{\sigma_\varepsilon}\right)\frac{\partial \varepsilon}{\partial z}\right] \quad (6)$$

Where,

$$G_k=\mu_t\{2\left[\left(\frac{\partial u}{\partial x}\right)^2+\left(\frac{\partial v}{\partial y}\right)^2+\left(\frac{\partial w}{\partial z}\right)^2\right]+\left(\frac{\partial u}{\partial y}+\frac{\partial v}{\partial x}\right)^2+\left(\frac{\partial u}{\partial z}+\frac{\partial w}{\partial x}\right)^2+\left(\frac{\partial v}{\partial z}+\frac{\partial w}{\partial y}\right)^2\} \quad (7)$$

$$\mu_t=\rho C_\mu\frac{k^2}{\varepsilon} \quad (8)$$

In Equations (1) – (8), *u, v,* and *w* represent the velocity in the *X*, *Y*, and *Z* direction, respectively, in units of m/s;

p is time-averaged pressure, in Pa;

μ and μ_t are the molecular viscosity coefficient and turbulence eddy viscous coefficient of the water, respectively, in m^2/s;

g is the acceleration of gravity in the *Z* direction, in m/s^2;

k is the turbulence kinetic energy, in m^2/s^2; *ε* is dissipation rate of the turbulence kinetic energy, in m^2/s^3;

σ_k and σ_ε are the Prandtl numbers corresponding to *k* and ε, respectively; $C_{1\varepsilon}$, $C_{2\varepsilon}$ and C_μ are empirical constants, with σ_k=1.0, σ_ε =1.3, $C_{1\varepsilon}$ =1.44, $C_{2\varepsilon}$ =1.92, and C_μ =0.09; and G_k is the generation term of the turbulence kinetic energy *k*, and it is caused by the mean velocity gradient.

Solution method and boundary conditions

The pressure implicit with splitting operators (PISO) method was used in this study, in which the "velocity inlet" is taken as the inlet boundary condition, and the value of the velocity is the average velocity taken from earlier experimental work [12]. The values of k and ε are taken as:

$$k=0.0144u_i^2 \quad (9)$$

$$\varepsilon=k^{0.5}/(0.5h_i) \quad (10)$$

In Equations (9) - (10), u_i and h_i are the velocity and the depth of the inlet, respectively. The hex-shaped grid was used in the entire model, and the time step was set as 0.002 s.

Mesh

In order to obtain a mesh-independent solution, a mesh-convergence analysis was carried out on the designs, and three block-structured meshes with different spatial resolutions were tested, namely Mesh-1, Mesh-2, and Mesh-3. The number of elements in each mesh was 48120, 95256, and 212254, and the average element size was 1.0067×10^{-3}, 5.032×10^{-4}, and 2.245×10^{-4} m^3. No significant differences were found in the results obtained using the two finer meshes (Mesh-2 and Mesh-3). Therefore, an average element size of 5.032×10^{-4} m^3 (Mesh-2) was adopted, with a slightly higher mesh density in the slot region.

RESULTS

In the case of gentle slope (S=2.6%, <10%), the main flow travels from one slot to the next through the pool as a two-dimensional curved flow [9][12]. Meanwhile, previous study has shown that the flow pattern in each pool is approximately the same for the most regular pools of the fishway, as mentioned before, and thus, Figures 2 (a) to (g) show the two-dimensional nephograms of the seven designs studied. Table 2 provides only the two-dimensional results of the third regular pool (pool 3) among the seven designs considered.

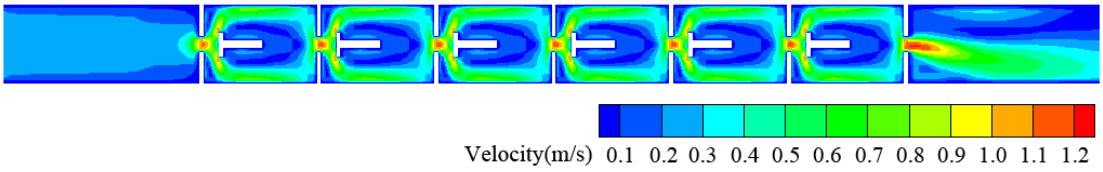

(a) - D1

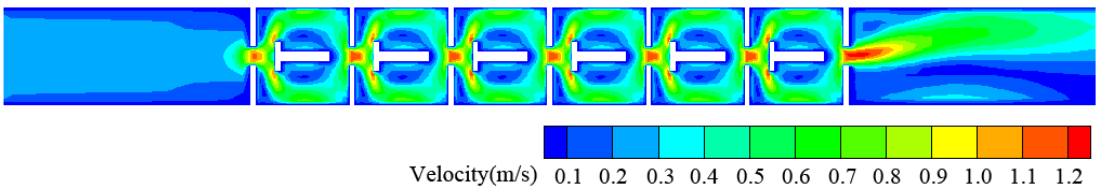

(b) - D2

Fig. 2 - Two-dimensional nephogram

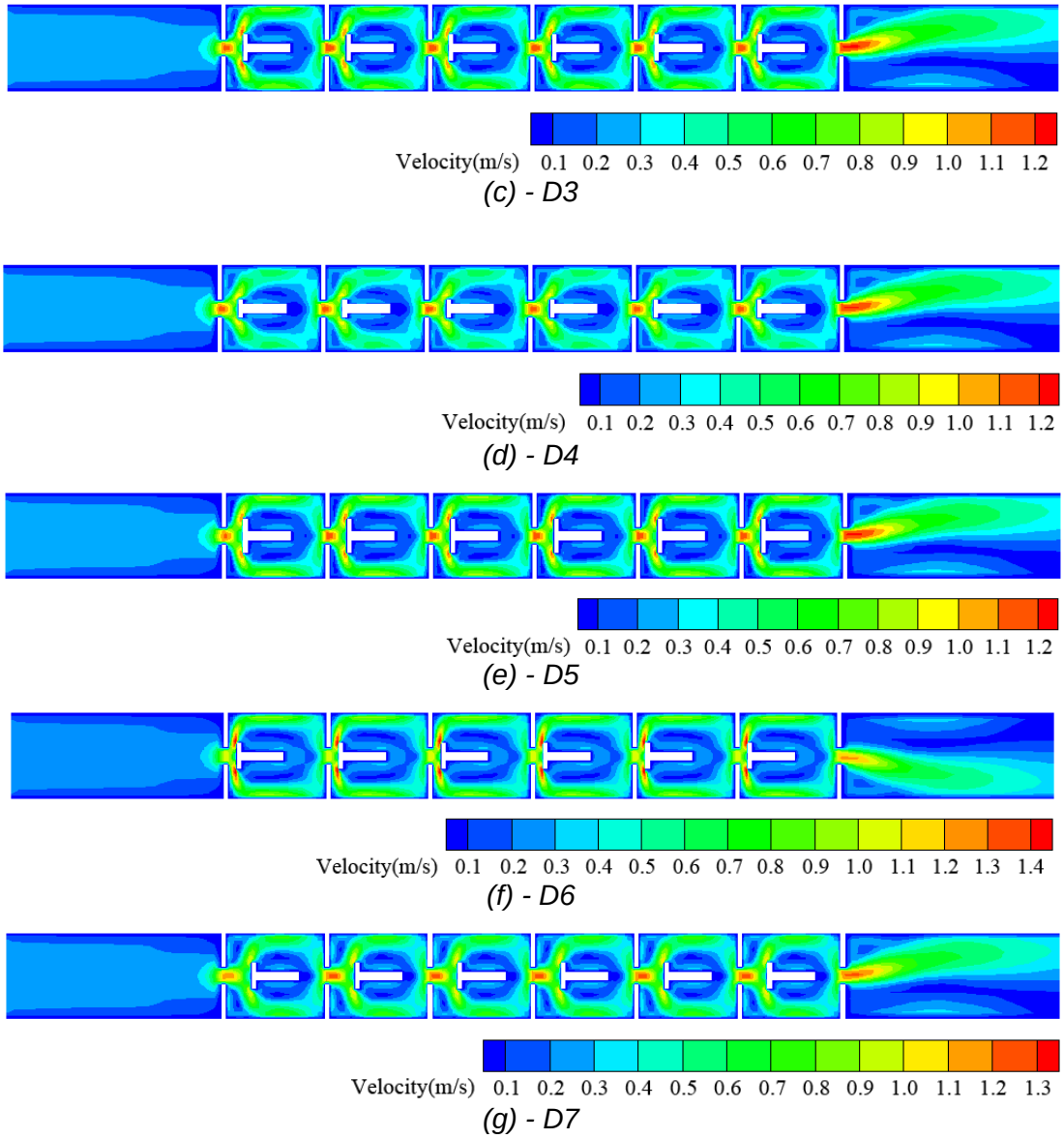

Fig. 2 - Two-dimensional nephogram

Under the given conditions, when the distance between the slot and the T lateral baffle was: (1) d=0.4 m (for D1–D5), the maximum velocity was approximately 1.2 m/s, as shown in Figure 2 (a)-(e); (2) d=0.2 m (for D6), the maximum velocity was approximately 1.4 m/s, as shown in Figure 2 (f); (3) d=0.6 m (for D7), the maximum velocity was approximately 1.3 m/s, as shown in Figure 2 (g).

Table 2 lists the two-dimensional results for pool 3, where X/b_s is the specific value between the X value and the width of the slot, b_s, V is the maximum velocity and the Y value indicates the location of V. V_a is the average velocity of the slot section (X=0), and V/V_a is the specific value between the maximum velocity of each section and the average velocity of the slot section.

According to the data of Table 2, the maximum velocity points in each column for the seven designs studied can be given, as shown in Figures 3 (a) and (b).

Tab. 2- Two-dimensional results of pool 3 in D1–D7 (D denotes "design")

D	V_a (m/s)	X (m)	Y (m)	V (m/s)	X/b_s	V/V_a	X (m)	Y (m)	V (m/s)	X/b_s	V/V_a
D1	1.03	0	1.12	1.04	0	1.01	0.5	0.61	1.08	1.25	1.05
		1	0.09	0.74	2.5	0.72	1.5	0.08	0.75	3.75	0.73
		2	0.08	0.67	5	0.65	2.5	0.08	0.49	6.25	0.48
D2	1.05	0	1.12	1.08	0	1.03	0.5	0.61	1.12	1.25	1.07
		1	0.09	0.76	2.5	0.72	1.5	0.08	0.62	3.75	0.59
		2	0.96	1.01	5	0.97	2.1	1.04	1.18	5.25	1.13
D3	1.03	0	1.12	1.05	0	1.02	0.5	0.61	1.1	1.25	1.07
		1	0.09	0.75	2.5	0.73	1.5	0.08	0.74	3.75	0.72
		2	0.08	0.48	5	0.47	2.5	0.96	1.16	6.25	1.13
D4	1.03	0	1.12	1.04	0	1.01	0.5	0.7	1.01	1.25	0.5
		1	0.11	0.51	2.5	0.5	1.5	0.13	0.53	3.75	0.52
		2	0.19	0.35	5	0.34	2.5	0.96	1.14	6.25	1.11
D5	1.03	0	1.12	1.05	0	1.02	0.5	0.53	1.05	1.25	1.02
		1	0.08	0.84	2.5	0.82	1.5	0.08	0.8	3.75	0.78
		2	0.07	0.54	5	0.52	2.5	0.96	1.16	6.25	1.13
D6	1.02	0	1.12	1.06	0	1.04	0.5	0.09	0.76	1.25	0.74
		1	0.08	0.97	2.5	0.95	1.5	0.08	0.89	3.75	0.87
		2	0.08	0.62	5	0.61	2.5	1.04	1.07	6.25	1.04
D7	1.05	0	1.12	1.07	0	1.02	0.5	0.95	0.81	1.25	0.78
		1	0.09	0.63	2.5	0.6	1.5	0.08	0.76	3.75	0.73
		2	0.08	0.52	5	0.5	2.5	0.96	1.2	6.25	1.15

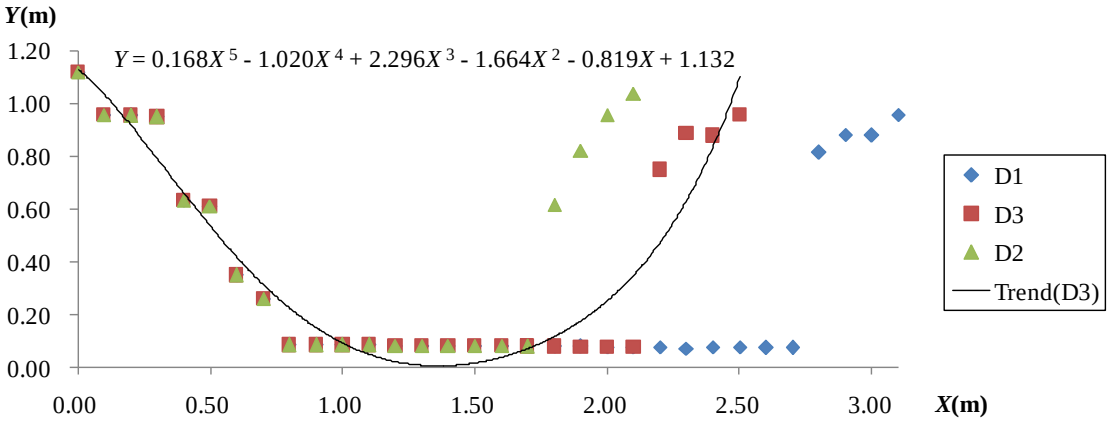

Fig. 3 (a) - Maximum velocity points in each column (D1–D3)

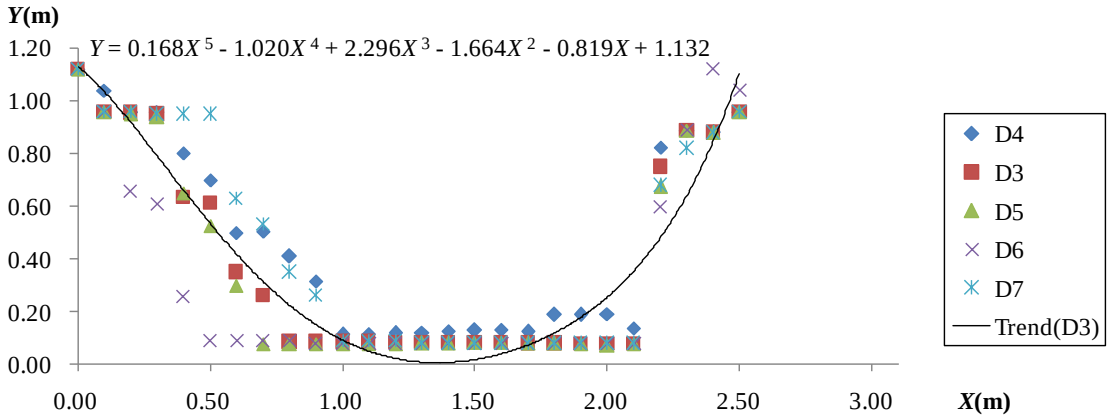

Fig. 3 (b) - Maximum velocity points in each column (D3–D7)

The trajectory equation of the maximum velocity line was defined to indicate the location of the maximum velocity (V) in each column. According to Table 2 and Figures 3 (a) and (b), the trajectory equation of the maximum velocity lines of the T shape fishways can be described as a "U" shape line, and can be expressed by the trend line of $D3$: $Y=0.168X^{5}-1.020X^{4}+2.296X^{3}-1.664X^{2}-0.819X+1.132$. The water is blocked by the T shape baffle after entering the slot of the regular pool, and then it symmetrically flows downstream from both sides of the T shape baffle.

According to the data of Table 2, the relationship between X/b_s and V/V_a can be given, as shown in Figures 4 (a) and (b).

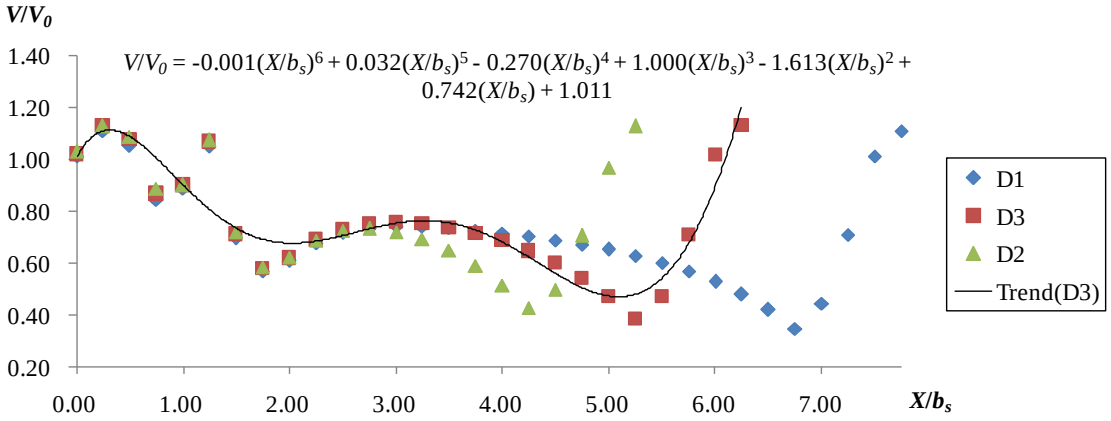

Fig. 4 (a) - Relationship between X/b_s and V/V_a (D1–D3)

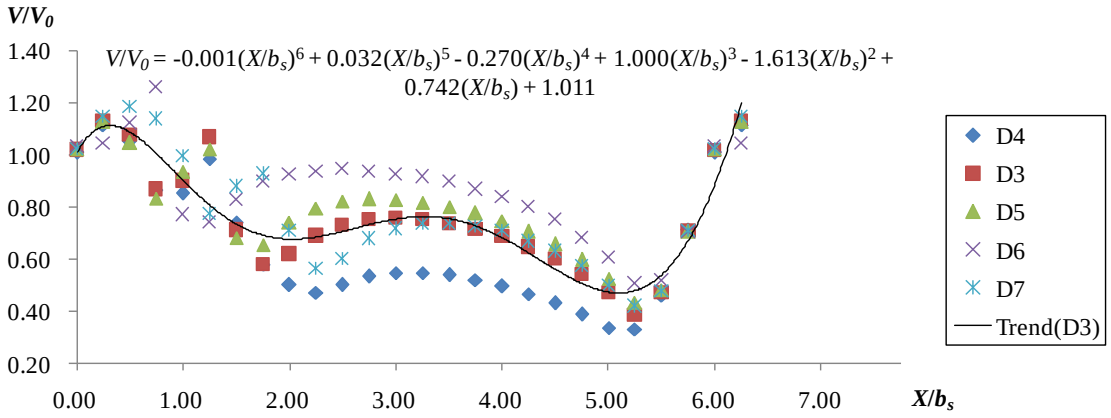

Fig. 4 (b) - Relationship between X/b_s and V/V_a (D3–D7)

The V/V_a equation was defined to indicate the ratio of the maximum velocity to the average velocity. According to Table 2 and Figure 4, the V/V_a equation of the T shape fishways can be described as a "W" shape line, and can be expressed by the trend line of *D*3: $V/V_a=-0.001(X/b_s)^6+0.032(X/b_s)^5-0.270(X/b_s)^4+1.000(X/b_s)^3-1.613(X/b_s)^2+0.742(X/b_s)+1.011$.

DISCUSSION

(1) The overall length of the seven designs was 24.5 m. According to Table 1, the length of the single regular pool of D3 was L=2.5 m, while the length of the single regular pool of D1 was L=3.0 m and the length of the single regular pool of D2 was L=2.0 m. As a result, the length of the transition pool of D3 was about 2 times that of the regular pool (about 4.8 m), while the length of the transition pool of D1 was approximately equal to the regular pool (about 3.2 m), and the length of the transition pool of D2 was about 3 times that of the regular pool (about 6.3 m). According to the literature [15], the appropriate size of the recirculation area can provide a resting place for fish, while an overly large area of recirculation will cause the fish to lose their way. Consequently, from Figures 2 (a)–(c) we can see, compared to D3 that the area of the recirculation zone in D1 was much larger and, in D2, was much smaller. Therefore, D3 is better than D1 and D2 in terms of the length of the regular pool.

(2) The length of the T lateral baffle was b_t=0.6, 0.4, and 0.8 m in D3, D4, and D5, respectively, as shown in Table 1. Figures 2 (c)–(e) show that the area of the recirculation zone in D4 was much

smaller compared to D3. The area of the recirculation zone in D5 was almost the same, compared to that in D3, but the cost of construction was greater than that of D3. Thus, D3 is better than D4 and D5 in terms of the length of the T lateral baffle, as well as in terms of the cost of construction.

(3) The distance between the slot and the T lateral baffle was d=0.4, 0.2, and 0.6 m in D3, D6, and D7, respectively, as shown in Table 1. Figures 2 (c), (f), and (g) show that the maximum velocity in D6 and D7 was larger than in D3. Therefore, D3 is better than D6 and D7 in terms of the distance between the slot and the T lateral baffle.

(4) The data in Table 2 and Figure 4 show that the maximum V/V_a was approximately 1.26 when X/b_s was approximately 0.75, which was near the T shape baffle; the minimum V/V_a was approximately 0.33 when X/b_s was approximately 5.25.

CONCLUSION

In this paper, the author presented the results of a numerical study of the hydraulics of T shape fishways that were constructed using seven different structural designs.

In the pools of T shape fishways, water is blocked by the T shape baffle after entering the slot of the regular pool, and then it symmetrically flows downstream from both sides of the T shape baffle.

The trajectory equation of the maximum velocity line of T shape fishways can be expressed as: $Y=0.168X^5-1.020X^4+2.296X^3-1.664X^2-0.819X+1.132$.

The V/V_a equation of T shape fishways can be expressed as: $V/V_a=-0.001(X/b_s)^6+0.032(X/b_s)^5-0.270(X/b_s)^4+1.000(X/b_s)^3-1.613(X/b_s)^2+0.742(X/b_s)+1.011$. Under the given conditions, the range of V/V_a was found to be between 0.33 and 1.26 ($0.33 \le V/V_a \le 1.26$); that is, for the seven different T shape fishway designs considered, the maximum and minimum values of the velocity can be calculated approximately as long as the average velocity of the slot section is known. In addition, the migratory requirements can be simultaneously checked, as to whether they satisfy the fish or not.

Of the seven designs studied, design 3 (D3) was found to be the most suitable design in terms of helping fish migrate the fishway efficiently. For D3, l_l=1.0 m, l_b=0.2 m, l_B=0.8 m, b_0=0.8 m, b_s=0.4 m, B=2.0 m, H=1.2 m, b_t=0.6 m, l_0=0.2 m, d=0.4 m, and L=2.5 m. According to the results, $d=b_s$, $b_t=1.5b_s$, $B=5b_s$, $L=6.25b_s$, and B/L= 4/5 are very satisfactory parameters for the dimensional design of T shape fishways.

ACKNOWLEDGEMENTS

This study was supported by Education Department of Sichuan Province (035Z1994), and by Sichuan Agricultural University (065H0600, 1921993122).

REFERENCES

[1] Food Agriculture Organization, 2002. Fish passes: design, dimensions and monitoring (Rome, FAO, in arrangement with DVWK) 119 pp.

[2] Mao X., 2018. Review of Fishway Research in China. Ecological Engineering, vol. 115: 91-95.

[3] Schwalme K., Mackay W., Lindner D., 2011. Suitability of Vertical Slot and Denil Fishways for Passing North-Temp, Canadian Journal of Fisheries & Aquatic Sciences, vol. 42: 1815-1822.

[4] Mallen-Cooper M., Stuart I., 2007. Optimising Denil fishways for passage of small and large fishes, Fisheries Management & Ecology, vol. 14: 61-71.

[5] Schwalme K., Mackay W. C., Lindner D., 1985. Suitability of Vertical Slot and Denil Fishways for Passing North-Temperate, Nonsalmonid Fish, Canadian Journal of Fisheries and Aquatic Sciences, vol. 42:1815-1822.

[6] Fuentes-Pérez J., Sanz-Ronda F., Azagra A., García-Vega A., 2016. Non-uniform hydraulic behavior of pool-weir fishways: a tool to optimize its design and performance, Ecological Engineering, vol. 86: 5-12.
[7] Larinier M. et al., 2002. Fishways: biological basis , design criteria and monitoring (Rome, FAO of the United Nations, DVWK) 208pp.
[8] Landsman S. J., Mclellan N., Platts J., Heuvel M., 2018. Nonsalmonid versus Salmonid Passage at Nature-Like and Pool-and-Weir Fishways in Atlantic Canada, with Special Attention to Rainbow Smelt, Transactions of the American Fisheries Society, vol. 147: 94-110.
[9] Wu S., Rajaratnam N., Katopodis C.,1999. Structure of Flow in Vertical Slot Fishway, Journal of Hydraulic Engineering, vol. 125: 351-360.
[10] Quaranta E., Katopodis C., Comoglio C., 2019. Effects of bed slope on the flow field of vertical slot fishways, River Research and Applications, vol. 35: 1-13.
[11] Stamou A. I., Mitsopoulos G., Rutschmann P., Bui M., 2018. Verification of a 3D CFD model for vertical slot fish-passes, Environmental Fluid Mechanics, vol. 18: 1435 –1461.
[12] Mao X., Fu J., Tuo Y., An R., Li J., 2012. Influence of structure on hydraulic characteristics of T shape fishway, Journal of Hydrodynamics, vol. 24: 684 – 691.
[13] John A., 1995. Computational fluid dynamics: the basics with applications (McGraw-Hill, New York, USA) 381pp.
[14] Oberkampf W. L., Trucano T. G., 2007. Verification and validation in computational fluid dynamics, Advances in Mechanics, vol. 38: 209-272.
[15] Mao X., 2015. Study of Fish-friendly Fishway Hydraulics in Mountainous Rivers of Southwest China (Sichuan University, Chengdu, China, in Chinese), PhD Thesis.